A human mutation in Phox2b causes lack of CO_2 chemosensitivity, fatal central apnea, and specific loss of parafacial neurons

Véronique Dubreuil*†, Nélina Ramanantsoa‡§, Delphine Trochet¶‖, Vanessa Vaubourg‡§, Jeanne Amiel¶‖, Jorge Gallego‡§, Jean-François Brunet*†**, and Christo Goridis*†**

*Ecole Normale Supérieure, Département de Biologie, 75005 Paris, France; †Centre National de la Recherche Scientifique, UMR8542, 75005 Paris, France; ‡Institut National de la Santé et de la Recherche Médicale, U 676, Hôpital Robert-Debré, 75019 Paris, France; §Université Paris 7-Denis Diderot, Faculté de Médecine, 75013 Paris, France; ¶Institut National de la Santé et de la Recherche Médicale, U 781, Hôpital Necker-Enfants Malades, 75743 Paris Cedex 15, France; and ‖Université Paris 5-René Descartes, Faculté de Médecine, Assistance Publique-Hôpitaux de Paris, 75006 Paris, France

Edited by Lynn T. Landmesser, Case Western Reserve University, Cleveland, OH, and approved December 10, 2007 (received for review September 27, 2007)

Breathing is maintained and controlled by a network of neurons in the brainstem that generate respiratory rhythm and provide regulatory input. Central chemoreception, the mechanism for CO_2 detection that provides an essential stimulatory input, is thought to involve neurons located near the medullary surface, whose nature is controversial. Good candidates are serotonergic medullary neurons and glutamatergic neurons in the parafacial region. Here, we show that mice bearing a mutation in *Phox2b* that causes congenital central hypoventilation syndrome in humans breathe irregularly, do not respond to an increase in CO_2, and die soon after birth from central apnea. They specifically lack Phox2b-expressing glutamatergic neurons located in the parafacial region, whereas other sites known or supposed to be involved in the control of breathing are anatomically normal. These data provide genetic evidence for the essential role of a specific population of medullary interneurons in driving proper breathing at birth and will be instrumental in understanding the etiopathology of congenital central hypoventilation syndrome.

brainstem | congenital central hypoventilation syndrome | neurodegenerative disease | respiration

Breathing is an integrated motor behavior that is driven by a respiratory rhythm generator located in the ventrolateral medulla. Stimulatory inputs from chemoreceptors that monitor CO_2 and O_2 in the blood provide a tonic drive to breathe and adapt it to exercise and the environment (1). There is general agreement that the main receptors sensing O_2 are located in the carotid body (CB), whereas responsiveness to CO_2/pH is mainly mediated by chemoreceptors in the brainstem. However, the nature of the primary central CO_2 sensors has not been firmly established. There also is disagreement as to whether central chemoreception is mediated by a small number of dedicated cells or is a widely distributed function of respiratory neurons. Nevertheless, a number of studies agree on the point that the essential CO_2 sensors are located close to the surface of the ventrolateral medulla (1). There are two main contenders for this role: serotonergic (5HT) medullary raphe neurons (2, 3) and the retrotrapezoid nucleus (RTN), a group of glutamatergic neurons located near the medullary surface ventral to the facial nucleus (nVII) (4, 5). The RTN neurons receive input from O_2-sensitive receptors in the CB via the nucleus of the solitary tract (nTS) and connect to the respiratory centers in the lower medulla (6, 7). Thus, they are in a position to integrate metabolic information on blood gases and to transmit this information to the respiratory centers. The RTN, which is mainly defined in the adult, overlaps anatomically with a potential oscillator network identified in neonates called the parafacial respiratory group (pFRG) (8, 9). It is still unclear to what extent both neuronal groups, collectively referred to as RTN/pFRG, are functionally and anatomically distinct.

Congenital central hypoventilation syndrome (CCHS) is a life-threatening genetic disease whose defining symptoms consist of respiratory arrest during sleep and a blunted or, in severe cases, an absent response to hypercapnia (10–12). The disease typically manifests itself at birth by hypoventilation or periods of apnea during sleep, but severely affected infants will never breathe properly whatever their state of arousal (10). Thus, understanding the molecular and cellular underpinnings of CCHS offers the promise of illuminating the mechanisms that are essential for CO_2 sensitivity and, more generally, proper breathing at birth. CCHS is known to be caused by heterozygous mutations of the PHOX2B transcription factor, mainly expansions of a polyalanine (polyAla) tract (13–15). The respiratory symptoms of CCHS patients point to a defect in the metabolic regulation of breathing and have been attributed to a failure of central chemosensory integration (11, 12), but the neural structures affected by the disease have remained obscure. Most infants with CCHS have no pathological lesions that are thought to be causal, although a bewildering variety of structures have been reported abnormal in some individuals (16–18).

To produce an animal model of CCHS in which to study the anatomical and physiological basis of the disorder, we have introduced into the mouse the most frequent *PHOX2B* mutation found in CCHS. As with the human patients, the mutant pups do not respond to hypercapnia, and they die soon after birth from central apnea. They specifically lack a population of glutamatergic Phox2b-expressing neurons in the RTN/pFRG region. This result strongly supports an essential role of these cells in sensing CO_2. In addition, the mutants have an irregular and slowed-down breathing pattern providing genetic evidence for the importance of the RTN/pFRG neurons for regular breathing at birth.

Results

Breathing Defects in *Phox2b*$^{27Ala/+}$ Mice. We have generated mice that bear the most frequent of the CCHS-causing mutations (14, 15), a +7 Alanine expansion of the 20-residues polyAla tract (the *Phox2b*^{27Ala} allele) by a knock-in approach (Fig. 1*A*). The heterozygous *Phox2b*$^{27Ala/+}$ offspring of the chimeric founders were born in Mendelian proportions (37 of 74 offspring of a chimera giving 100% transmission), but they suffered from gasping behavior and cyanosis and died in the first hours after birth from respiratory failure (Fig. 1*B*). Plethysmographic recordings performed immediately after delivery showed a range of phenotypes in mutant pups breathing

Author contributions: V.D. and N.R. contributed equally to this work; J.-F.B. and C.G. contributed equally to this work; V.D. and N.R. designed research; V.D., N.R., D.T., and V.V. performed research; J.A., J.G., J.-F.B., and C.G. analyzed data; and C.G. wrote the paper.

The authors declare no conflict of interest.

This article is a PNAS Direct Submission.

**To whom correspondence may be addressed. E-mail: jfbrunet@biologie.ens.fr or goridis@biologie.ens.fr.

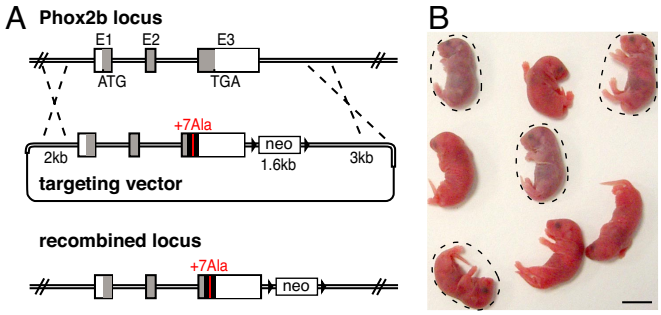

Fig. 1. Generation of *Phox2b*$^{27Ala/+}$ mutants. (*A*) Schematic representation of the wild-type *Phox2b* locus, the targeting vector, and the recombined locus. E1, exon 1; E2, exon 2. With the coding regions in gray, the human DNA fragment is highlighted in black, and the extended polyAla tract is in red. neo, *neomycin* resistance cassette; black triangles, *loxP* sites. (*B*) Offspring of a founder chimera immediately after birth. Mutants are encircled. (Scale bar: 1 cm.)

normal air. Three of 18 mutants analyzed ventilated only by intermittent gasping. The remaining mutants showed a continuum of phenotypes, some breathing quite rhythmically but at a slower rate, whereas the breathing of others was chaotic and interrupted by periods of apnea (Fig. 2*A*). As a consequence, the mean respiratory minute volume (VE) measured during apnea-free periods of fairly eupnoeic pups was depressed in the mutants (Fig. 2*B*). When quantified by measuring the variability of interbreath intervals, breathing irregularity, expressed as the percent coefficient of variance, was found to be significantly greater for mutant than for wild-type pups [73 ± 7% and 56 ± 4%, respectively, during the first 5 min in normal air ($P = 0.026$); 101 ± 10% and 65 ± 4.4%, respectively, during the last 5-min period of the recording ($P = 0.003$; mean ± SEM)]. Short apneic episodes also occurred in wild-type neonates, but they were more frequent and lasted longer in the mutants, resulting in a 6.5-fold higher total apnea duration (Fig. 2 *A* and *C*). Fully penetrant was a lack of the normal response to hypercapnia (i.e., an increase in both respiratory frequency and amplitude), indicating that central chemoreception was defective (Fig. 2 *A* and *D*). By contrast, the newborn mutants appeared histopathologically normal by gross inspection, and their body weight and temperature did not differ significantly from that of the wild-type pups (data not shown). Thus, *Phox2b*$^{27Ala/+}$ mice resemble severe cases of CCHS and share the cardinal symptom of the disease, a lack of response to hypercapnia.

Specific Loss of Parafacial Interneurons in *Phox2b*$^{27Ala/+}$ Mice. The severe phenotype suggested to us that an important respiratory center was defective in the mutants. Given that the mutant allele is expressed from the *Phox2b* locus, the location of the defect should be sought primarily in *Phox2b*-expressing structures, although we cannot exclude that *Phox2b*-negative respiratory neurons are secondarily affected by a non-cell-autonomous mechanism. Excellent candidates were the Phox2b-expressing glutamatergic (*vGlut2*$^+$) neurons robustly activated by hypercapnia that have recently been identified in the RTN/pFRG region of the adult rat (7). Accordingly, we identified neurons coexpressing *Phox2b* and *vGlut2* in newborn mice at a similar location close to the medullary surface, ventral and caudal to nVII. In newborn [postnatal day 0 (P0)] *Phox2b*$^{27Ala/+}$ mutants, these cells were severely depleted (Fig. 3 *A* and *B*). For quantification, we separated the *Phox2b*$^+$;*vGlut2*$^+$ RTN/pFRG cells into two groups that we could anatomically distinguish: those ventral to nVII and those forming a compact group immediately caudal to it. Their numbers were reduced by 77% and 54%, respectively (Fig. 3*G*). Prompted by previous work suggesting that neurokinin-1 receptor (NK1R)-positive neurons in the RTN participate in CO_2 sensitivity (4), we examined NK1R expression. In newborn mutants, the NK1R immunoreactivity

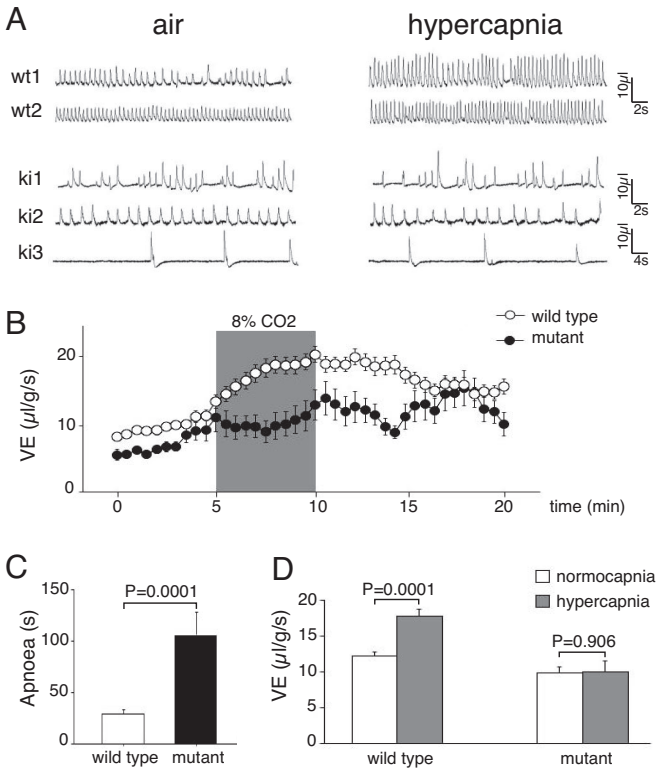

Fig. 2. Disrupted breathing in *Phox2b*$^{27Ala/+}$ mice. (*A*) Representative examples of plethysmographic recordings of wild-type (wt) and *Phox2b*$^{27Ala/+}$ (ki) littermates breathing normal or hypercapnic air during the first 20 min after delivery. (*B*) Ventilatory (VE) tracings of *Phox2b*$^{27Ala/+}$ (black dots) pups and their wild-type (white dots) littermates breathing air or hypercapnic mixture (8% CO_2; shaded area). Periods of apnea and animals respirating mainly by gasps were excluded from the analysis. Each dot represents the mean ± SEM over a 30-sec period ($n = 15$ and $n = 43$ for mutant and wild-type pups, respectively) (when no bar is visible, it was smaller than the diameter of the dot). Baseline ventilation in air was depressed in the mutants, which did not increase VE during hypercapnia. Ventilation increased in both mutant and wild-type pups during the first 5 min in normal air because of increases in tidal volume and breathing frequency. Numerous mechanisms that operate immediately after delivery may account for this phenomenon. Among these mechanisms, the increase in lung compliance secondary to liquid resorption is accompanied by a progressive increase in tidal volume. Also in human infants, breathing becomes progressively more rapid and deeper after the first breaths (50). (*C*) Total apnea duration (sec) summed over the 5-min period in air for wild-type ($n = 43$) and *Phox2b*$^{27Ala/+}$ ($n = 15$) pups, excluding those that respirated only by gasping (mean ± SEM). (*D*) Average VE for wild-type ($n = 43$) and *Phox2b*$^{27Ala/+}$ ($n = 15$) pups breathing normal or hypercapnic air. Normocapnic values were calculated as the mean value over the first 5 min and the last 5 min of the recording to take into account the overall increase in VE. Hypercapnic VE values were calculated as the mean values over the last 3 min of hypercapnic exposure. In contrast to wild-type pups, the mutants did not significantly increase their ventilation in response to elevated pCO_2.

normally highly concentrated at the medullary surface was almost abrogated, and very few Phox2b;NK1R-double-positive cells remained (Fig. 3 *C* and *D*). To exclude that the defect was secondary to hypoxia experienced after birth, we investigated whether the RTN/pFRG might be defective already in the embryo. We identified RTN/pFRG neurons by double staining for NK1R and Phox2b because *vGlut2* expression was weak before birth. At embryonic day 15.5 (E15.5), NK1R immunoreactivity was already severely curtailed in the RTN/pFRG (Fig. 3 *E* and *F*), but was preserved at other locations (data not shown). The number of cells double-positive for NK1R and Phox2b was reduced by 70%, both ventral

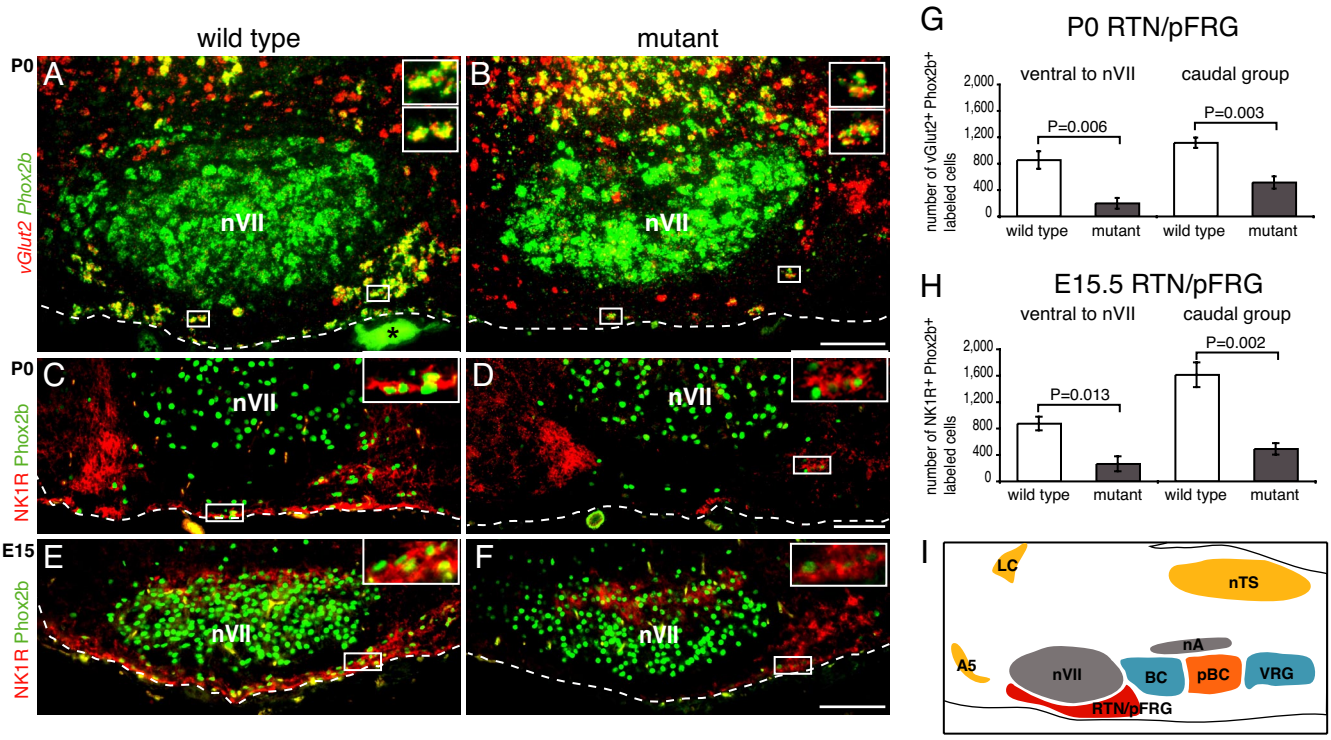

Fig. 3. Loss of RTN/pFRG neurons in *Phox2b*$^{27Ala/+}$ mice. (*A* and *B*) *In situ* hybridization with *Phox2b* (green) and *vGlut2* (red) probes on sections of P0 wild-type (*A*) and mutant (*B*) brains. The double-positive RTN neurons ventral and caudal to nVII are severely reduced in the mutants (see *G* for quantification), whereas double-positive cells persist in normal numbers dorsal to nVII (2,166 ± 219 and 2,410 ± 276, mean ± SEM, for four wild types and four mutants, respectively; $P = 0.52$). The asterisk indicates a nonspecific signal from a blood vessel. (*C–F*) Loss of Phox2b (green) and NK1R (red) double-positive cells in the RTN/pFRG from P0 (*C* and *D*) and E15.5 (*E* and *F*) wild-type (*C* and *E*) and mutant (*D* and *F*) brains. (*Insets*) Enlargements of the framed regions. The dashed lines mark the medullary surface. Sagittal sections are shown. Rostral is left and dorsal is up. (Scale bars: 0.1 mm.) (*G*) Counts of *Phox2b*$^{+}$;*vGlut2*$^{+}$ cells (mean ± SEM for four pups of each genotype). (*H*) Counts of Phox2b^{+};NK1R^{+} cells (mean ± SEM for three *Phox2b*$^{+/+}$ and four *Phox2b*$^{27Ala/+}$ embryos) in the RTN/pFRG, done separately for the cells ventral to nVII and for those in an adjacent compact group caudal to it. (*I*) Schematic representation of the principal neuronal groups involved in respiration and the landmarks referred to in the text on a sagittal section of the mouse brainstem. A5, noradrenergic cell group A5; BC, Bötzinger complex; LC, locus coeruleus; nA, nucleus ambiguous; nTS, nucleus of the solitary tract; pBC, pre-Bötzinger complex; RTN/pFRG, retrotrapezoid nucleus/parafacial respiratory group; VRG, ventral respiratory group.

to nVII and in the group of Phox2b^{+}, NK1R^{+} neurons immediately caudal to it (Fig. 3*H*).

We next examined other Phox2b-expressing structures, which are known to play a role in respiratory control: the CB, a peripheral chemoreceptor organ monitoring pO_2 and pCO_2 in the blood, but thought to mediate mainly the response to hypoxia (19); the petrosal/nodose ganglionic complex (gIX/X) that conveys sensory information from the CB to the brain (20) and contains the cell bodies of pulmonary stretch receptors; the locus coeruleus (LC), which stimulates respiration in newborn mice (21); and the A5 cell group that exerts an inhibitory influence on respiration (21). The CB, the gIX/X, and the LC analyzed on histological sections appeared normal in *Phox2b*$^{27Ala/+}$ neonates (Fig. 4 *A–F*). The glomus cells in the CB and the gIX/X and LC neurons were present in normal numbers (Fig. 4*M*). The LC also appeared normal by tyrosine hydroxylase (TH) immunohistochemistry (Fig. 4 *G* and *H*), which also was used to reveal the noradrenergic neurons of the A5 cell group, whose numbers did not differ significantly between both genotypes (Fig. 4 *I*, *J*, and *M*). Finally, we examined the nTS that transmits sensory input from peripheral chemoreceptors by Phox2b immunohistochemistry. It also was not detectably altered (Fig. 4 *K* and *L*) (data not shown).

We then analyzed two Phox2b-negative cell groups that are essential for normal breathing: the pre-Bötzinger complex (pre-BötC), a region critical for respiratory rhythm generation (22, 23), and the medullary 5HT neurons, which have been proposed as a principal site of CO_2 chemoreception (2) and are important modulators of respiration (24). In neonatal rodents, the preBötC has been anatomically defined by its location ventral to the nucleus ambiguus (nA) and its expression of NK1R (25, 26). We identified an NK1R-positive region at the appropriate location ventral to nA (distinguished from the preBötC by its positivity for Phox2b) (data not shown) that contained clearly discernible NK1R-positive cell bodies. A very similar pattern of NK1R staining was found in the *Phox2b*$^{27Ala/+}$ mutants (Fig. 5 *A* and *B*). The medullary 5HT neurons were preserved in the mutants (Fig. 5 *C* and *D*) and were present in normal numbers in both the medullary raphe and the ventrolateral medulla (Fig. 5*E*). In summary, with the exception of the RTN/pFRG, we did not detect anatomical defects of the principal neuronal groups involved in the control of respiration, although we cannot exclude more subtle functional alterations.

Discussion

A Mouse Model of Congenital Central Hypoventilation Syndrome. The onset of breathing at birth is an important adaptation to extrauterine life, and irregular and instable respiration at birth is not uncommon and is characteristic for preterm infants. Several mouse mutants with breathing defects that result from abnormal brainstem development and lead to neonatal death have been proposed as models to study the functional anatomy of the respiratory circuits. *Egr2*$^{-/-}$ (27), *Hoxa1*$^{-/-}$ (28), and *Tlx3*$^{-/-}$ (29, 30) mice have extensive abnormalities in the pons and the medulla, and it may prove difficult to relate their phenotypes to a precise anatomical lesion. Impaired respiration in *Phox2a*$^{-/-}$ mice has been attributed to the loss of the LC (31), but atrophy of the gIX/X also may be involved (32). In *MafB* mutants, most brainstem structures

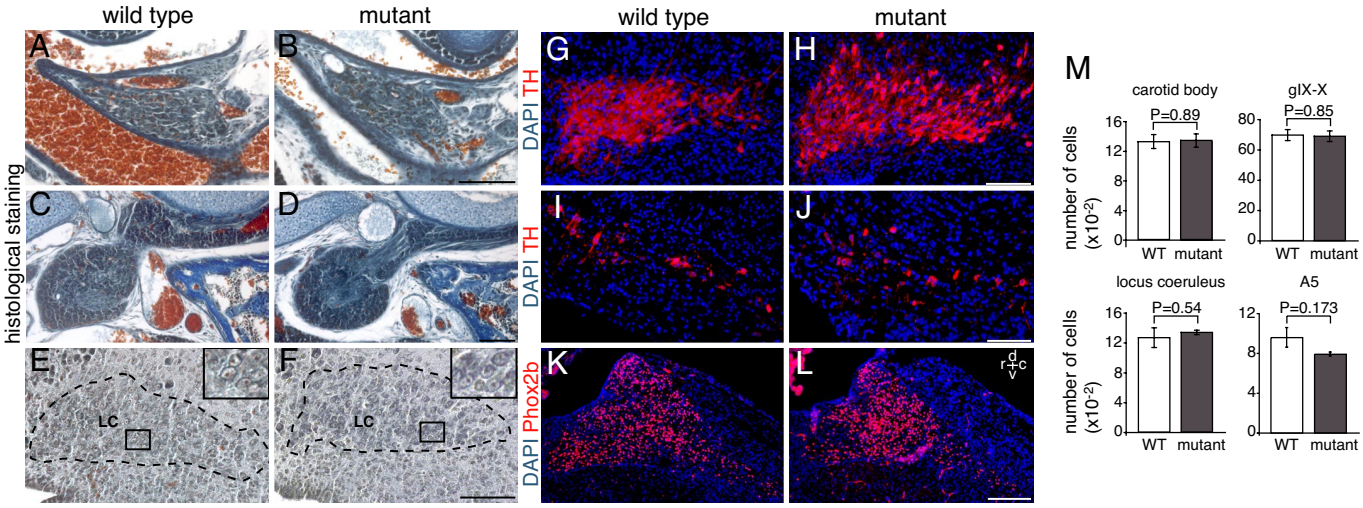

Fig. 4. Analysis of structures that depend on *Phox2b* for proper development and are involved in respiratory control in *Phox2b*$^{27Ala/+}$ and *Phox2b*$^{+/+}$ neonates. (*A–D*) The CB is preserved in newborn mutants (*A* and *B*), as is the petrosal/nodose (gIX/X) ganglionic complex (*C* and *D*). (*E–H*) The LC appears normal by histology (*E* and *F*) and TH immunohistochemistry (*G* and *H*) in the mutants. In *E* and *F*, the LC is encircled by a dashed line. (*Insets*) Enlargements of the framed areas showing the typical large LC neurons that were counted. (*I* and *J*) The noradrenergic neurons of the A5 cell group are detected in similar numbers by TH immunohistochemistry in wild-type and mutant neonates. (*K* and *L*) As assessed by Phox2b immunohistochemistry, the nTS is not detectably altered in *Phox2b*$^{27Ala/+}$ mutants. Sagittal sections are shown (Scale bars: *B*, *D*, *F*, *H*, and *J*, 0.1 mm; *L*, 0.2 mm.) (*M*) Counts of glomus cells in the CB, of gIX/X and LC neurons, and of A5 cells. The estimated cell number per animal is given (mean ± SEM for three pups of each genotype).

appeared normal, and their respiratory failure has been ascribed to the disruption of the preBötC (33). The absence of BDNF also results in depressed and irregular breathing (34), which can be attributed to impaired peripheral chemoreception, although a loss of A5 neurons also has been described (35). In *Phox2a*, *BDNF*, or *MafB* mutants, the respiratory responses to pO_2 are altered, but a blunted response to hypercapnia indicative of impaired central chemosensitivity was not reported for any of the mutants.

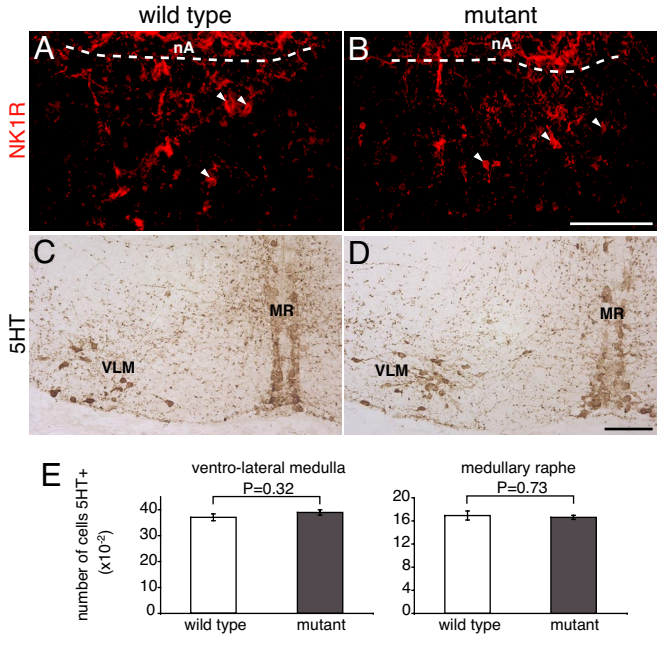

Fig. 5. Analysis of the preBötC and of 5HT neurons. (*A* and *B*) The preBötC complex was visualized by NK1R immunohistochemistry on sagittal sections of *Phox2b*$^{27Ala/+}$ and *Phox2b*$^{+/+}$ neonates. The arrowheads point to NK1R^{+} cell bodies. A dashed line delimits the caudal border of the nA. (Scale bar: 0.1 mm.) (*C* and *D*) The medullary 5HT neurons were visualized by 5HT immunocytochemistry on coronal section of E15.5 *Phox2b*$^{27Ala/+}$ and *Phox2b*$^{+/+}$ embryos. MR, medullary raphe; VLM, ventrolateral medulla. (*E*) Quantification of 5HT neurons. The number of 5HT-expressing cells per animal did not differ significantly between *Phox2b*$^{27Ala/+}$ and wild-type embryos (mean ± SEM for three pups of each genotype).

CCHS provides an experiment of nature, which has the potential to resolve some of the uncertainties that surround the control of breathing in the perinatal period. To produce an authentic model of CCHS, we generated mice bearing the most frequent CCHS-causing mutation. The *Phox2b*$^{27Ala/+}$ mice reproduce the phenotype of severe cases of CCHS and a key symptom of the disease, a defective response to hypercapnia. They thus represent a valid model of CCHS for future mechanistic studies. We searched for anatomical defects in the structures that have been implicated in the control of respiration. The only alteration we found in the mutants was the depletion of a set of interneurons in the RTN/pFRG region, a previously proposed principal site of CO_2 sensitivity (4, 5). Thus, the respiratory failure of *Phox2b27*$^{Ala/+}$ pups is most easily explained by the loss of Phox2b-expressing RTN/pFRG interneurons, although we cannot exclude more subtle functional deficits at other sites involved in respiratory control. These data, by guiding anatomical and imaging studies in the patients, may lead to the identification of the human equivalent of the RTN/pFRG, which still needs to be defined. Moreover, our mouse mutants will enable us to study the developmental history of the demise of the RTN/pFRG neurons and the reason for their vulnerability. In fact, the reasons for the selective vulnerability of some neuronal types and the resistance of others that also express the mutant protein are not understood for any of the polyAla expansion disorders (36, 37). Finally, because heterozygous *Phox2b*-null mutants have only a mild and transient breathing defect (38), the results at hand demonstrate already that the respiratory failure of *Phox2b*$^{27Ala/+}$ mutants and by extrapolation of CCHS patients is caused by a toxic gain of function or a dominant-negative effect, not by haploinsufficiency.

Role of Parafacial Neurons in Respiratory Control. The location and phenotype of the neurons that are the central CO_2 sensors and primary respiratory rhythm generators *in vivo* are still a matter of debate. The RTN and pFRG are two groups of neurons in the parafacial region that have been functionally defined as chemosen-

sitive and rhythmogenic, respectively, but overlap anatomically (4, 5, 8, 9).

The RTN was initially identified as a region that innervates the respiratory neurons in the lower medulla (6). It has been subsequently shown to be a chemoreceptor site (4, 39), culminating with the observation that it contains neurons robustly activated by CO_2 in the adult rat *in vivo* (5). We found neurons expressing the same molecular phenotype as the previously described CO_2-sensing RTN neurons (7) at an equivalent location in the newborn mouse, and these neurons were selectively depleted in the *Phox2b*$^{27Ala/+}$ neonates, which are unable to respond to hypercapnia. Hence, the depletion of RTN neurons in *Phox2b27*$^{Ala/+}$ mice likely causes the lack of response to hypercapnia. These data highlight the critical importance of the RTN for CO_2 sensitivity among the known or hypothesized central chemoreceptor sites.

The ataxic breathing pattern and the gasping behavior of the *Phox2b*$^{27Ala/+}$ mutants leading to fatal central apnoea are most easily explained by positing that adequate respiration at birth depends on the excitatory drive afforded by CO_2 sensors in the RTN. Because the pFRG that has been implicated in respiratory rhythm generation in newborn rodents is anatomically coextensive with the RTN, it remains possible that the Phox2b$^+$ neurons missing in the mutants have a more direct role in rhythm generation. Whatever the case, our results provide genetic evidence for an essential role of the RTN/pFRG in the control of breathing in the critical neonatal period.

Breathing is known to mature postnatally (1), such that respiratory distress at birth caused by genetic alterations may be alleviated at later stages (27, 38). Thus, the respiratory control mechanisms at fault in *Phox2b*$^{27Ala/+}$ mutants may become less critical for survival at later stages. However, they may remain crucial during sleep because, past the newborn period, most CCHS patients are able to sustain normal gas exchange when awake, but need respiratory assistance when asleep (10, 40). Furthermore, the mechanisms defective in our mouse mutants may again become essential in periods of respiratory distress due to other insults. For instance, there are now several cases of patients with mutations in *PHOX2B*, which present later in life with typical CCHS symptoms triggered by upper airway infections (41).

Recent *in vivo* and *in vitro* experiments have provided important insights into the sites and mechanisms that underlie adequate breathing in mammals. Still, a consensus as to which are essential in different conditions has yet to emerge. Our results indicate the vital function of a group of parafacial interneurons in one of these conditions, the onset of regular breathing at birth, and highlight the potential of the CCHS-causing *Phox2b* mutations for analyzing the neuronal circuits that control respiration.

Materials and Methods

Mice. A DNA fragment surrounding the polyAla tract and extending from a SacI site found at the same location in mouse and human exon 3 up to the stop codon was amplified from the genomic DNA of a patient with the +7 Ala expansion. It replaces the corresponding mouse sequence in the 5′ homology arm of the targeting vector. Because human and mouse Phox2b proteins are identical in sequence, the encoded protein is identical to mouse Phox2b except for an extension of the polyAla tract by seven additional residues. The targeting vector contains in addition a *neomycin* resistance cassette (*neo*) flanked by *loxP* sites and the 3′ homology arm (Fig. 1*A*). Correctly recombined ES cells were obtained by electroporation of P1 (129 S2/SvPas) ES cells. Injection of each of three clones into C57BL/6 blastocysts yielded chimeric founders, of which five gave rise to ES cell-derived offspring after mating with C57BL/6 mice. The chimeric founders were produced at the Mouse Clinical Institute/Institut Clinique de la Souris (Illkirch, France; http://www-mci.u-strasbg.fr). Genotyping was done by PCR on tail DNA with primers surrounding the polyAla tract, but no mutant offspring were found at weaning (0 of 53 agouti mice derived from two independent recombination events, of a total of 496 offspring). To exclude the possibility that the presence of *neo* may contribute to the phenotype, the founders were mated with *Pgk-cre* deleter (42) females. We did not find any phenotypic differences between pups, which harbored the *neomycin* cassette and those that did not (data not shown). We thus pooled the results obtained with mice born of *Pgk-cre* or B6D2 wild-type females. The day of the vaginal plug was considered as E0.5. Delivery took place between E18.5 and E19. All animal studies were done in accordance with the guidelines issued by the French Ministry of Agriculture and have been approved by Direction Départementale des Services Vétérinaires de Paris.

Plethysmography. Breathing movements were recorded noninvasively in unanaesthesized, unrestrained pups within 20 min after delivery, using whole-body flow barometric plethysmography as described (43, 44). A constant bias flow (200 ml/min) prevented CO_2 and water accumulation and ambient temperature drifts over time. After 5 min in room air, the pups were exposed to hypercapnic (8% CO_2/21% O_2/71% N_2) air, followed by 10 min in air. Apnoeas, defined as ventilatory pauses longer than twice the duration of the preceding breath, were determined by using an automatic classification method (43). Breathing variables [breath duration (T_{TOT}), tidal volume (V_T), and ventilation (V_E) calculated as V_T/T_{TOT}] were measured on apnea-free periods. Pups respirating only by gasps were excluded from the analysis. The data were obtained by analyzing 15 mutant and 43 wild-type pups. In all cases, statistical analysis was done by using Statview5 with the α-level set at 0.05. To calculate the data shown in Fig. 2*D*, ventilation was measured by using repeated-measures ANOVA with genotype (mutant vs. wild-type mice) and gas (air vs. hypercapnia) as a repeated factor. A two-tailed *t* test was used in all other cases.

Histology. Serial 14-μm sections of P0 mice were prepared for plain histology and stained with Groat's hematoxylin and Mallory's trichrome as described in ref. 32. The number of glomus cells in the carotid body and of neurons in the LC and in gIX/X was estimated by counting large (>10-μm) nuclei containing at least one distinct nucleolus on sagittal or coronal sections. Nuclear profiles were counted in every other section for the LC and the carotid body, in every fourth section for gIX/X. Cells were counted on both sides and their total number estimated by multiplication by 2 or 4. The longest diameters of randomly selected 50 nuclei were measured by using ImageJ on sections cut at right angles to the plane of the section counted (45). The mean values obtained were not found to differ significantly between wild-type and mutant mice, and there were no visible differences in shape and orientation of the nuclei. From this result, we concluded that the accuracy of cell counts was similar in wild-type and mutant animals and that the raw counts could be compared without correction (46).

For *in situ* hybridization and immunohistochemistry, brains were fixed in 4% paraformaldehyde and analyzed on sagittal or coronal cryosections of 12 μm. Fluorescent *in situ* hybridization with *vGlut2* and *Phox2b* riboprobes labeled with digoxygenin (DIG) and FITC, respectively, was done as described (47, 48). Briefly, the sections were hybridized simultaneously with both probes, followed by sequential incubations with horseradish peroxidase-coupled anti-FITC Fab and FITC-tyramide working solution (PerkinElmer). After removal of the anti-FITC antibodies by incubation for 10 min in 50% formamide, 2× SSC, and 0.1% Tween 20 at 70°C, the DIG-labeled probe was detected by incubation with horseradish-coupled anti-DIG Fab fragments, followed by incubation with Cy3-tyramide working solution (PerkinElmer). Antibodies used for immunohistochemistry were rabbit (49) or guinea pig (a kind gift of H. Enomoto, RIKEN Center for Developmental Biology, Hyogo, Japan) anti-Phox2b, rabbit anti-NK1R (Abcam), rabbit anti-TH (Sigma–Aldrich), and rabbit anti-5HT (Sigma–Aldrich) that were revealed with fluorescent Alexa488- or Cy3-coupled secondary antibodies (Jackson Laboratories) or with a Vectastain ABC kit (Vector Laboratories). Double-labeled *Phox2b*$^+$;*vGlut2*$^+$ or Phox2b$^+$;NK1R$^+$ neurons were counted on every sixth sagittal section, within an area (7) delimited ventrally by the medullary surface, dorsally by nVII, rostrally by the rostral end of nVII, and extending for 0.125 mm caudal to nVII. *Phox2b*$^+$;*vGlut2*$^+$ cells dorsal to nVII were counted in a rectangle drawn parallel to the surface of the medulla on every fourth section. For counting A5 neurons, TH$^+$ cells were counted on every fourth section in a small rectangle over the entire length of this cell group. The number of medullary 5HT neurons was estimated by counting 5HT$^+$ cells on coronal sections throughout the caudal serotonergic cluster. They were separated into two groups: those neurons located within the midline raphe (N. raphe pallidus, raphe obscuru, and raphe magnus) and those neurons located in the ventrolateral medulla and in the paragigantocellular reticular nucleus. In all cases, cells were counted on both sides, and the total number of cells estimated by multiplication by 4 or 6.

Statistical analysis was done by using a two-tailed *t* test and XLSTAT software, with the α-level set at 0.05. The values were found to be normally distributed (Shapiro–Wilk and Lilliefors tests) and the variances to be equal (Fisher's *F* test) in all cases. Pictures were taken with a Leica DC 300F or 350F camera mounted on a

Leica DMRXA2 microscope and Leica QFluoro software and were processed by Adobe Photoshop (Adobe Systems).

ACKNOWLEDGMENTS. We thank P. Guyenet (University of Virginia, Charlottesville, VA) for the *vGlut2* probe, H. Enomoto (RIKEN Center for Developmental Biology, Hyogo, Japan) for anti-Phox2b antibodies, B. Matrot and G. Vardon for developing the plethysmographic system, and S. Dauger for help with experiments. The *Phox2b*^{27Ala} chimeras were produced at the Mouse Clinical Institute (Illkirch, France) with funds from the GIS ''Maladies Rares'' (J.A.). This work was supported by the Agence Nationale de la Recherche (J.-F.B. and J.A.), the Fondation pour la Recherche Médicale (J.F.-B. and D.T.), the Association Française contre les Myopathies (C.G.), the Chancellerie des Universités de Paris (Legs Poix) (J.G.), the Association pour la Recherche sur le Cancer (V.D.), the Société de Pneumologie de Langue Française, the Association Française du Syndrome d'Ondine, and Fondation Garches (N.R.).

1. Feldman JL, Mitchell GS, Nattie EE (2003) Breathing: Rhythmicity, plasticity, chemosensitivity. *Annu Rev Neurosci* 26:239–266.
2. Richerson GB (2004) Serotonergic neurons as carbon dioxide sensors that maintain pH homeostasis. *Nat Rev Neurosci* 5:449–461.
3. Richerson GB, Wang W, Hodges MR, Dohle CI, Diez-Sampedro A (2005) Homing in on the specific phenotype(s) of central respiratory chemoreceptors. *Exp Physiol* 90:259–266.
4. Nattie EE, Li A (2002) Substance P-saporin lesion of neurons with NK1 receptors in one chemoreceptor site in rats decreases ventilation and chemosensitivity. *J Physiol* 544:603–616.
5. Mulkey DK, *et al*. (2004) Respiratory control by ventral surface chemoreceptor neurons in rats. *Nat Neurosci* 7:1360–1369.
6. Smith JC, Morrison DE, Ellenberger HH, Otto MR, Feldman JL (1989) Brainstem projections to the major respiratory neuron populations in the medulla of the cat. *J Comp Neurol* 281:69–96.
7. Stornetta RL, *et al*. (2006) Expression of Phox2b by brainstem neurons involved in chemosensory integration in the adult rat. *J Neurosci* 26:10305–10314.
8. Onimaru H, Homma I (2003) A novel functional neuron group for respiratory rhythm generation in the ventral medulla. *J Neurosci* 23:1478–1486.
9. Onimaru H, Homma I (2006) Point:Counterpoint: The parafacial respiratory group (pFRG)/pre-Bötzinger complex (preBötC) is the primary site of respiratory rhythm generation in the mammal. *J Appl Physiol* 100:2094–2095.
10. Gozal D (1998) Congenital central hypoventilation syndrome: An update. *Pediatr Pulmonol* 26:273–282.
11. Spengler CM, Gozal D, Shea SA (2001) Chemoreceptive mechanisms elucidated by studies of congenital central hypoventilation syndrome. *Respir Physiol* 129:247–255.
12. Chen ML, Keens TG (2004) Congenital central hypoventilation syndrome: Not just another rare disorder. *Paediatr Respir Rev* 5:182–189.
13. Amiel J, *et al*. (2003) Polyalanine expansion and frame shift mutations of the paired-like homeobox gene PHOX2B in congenital central hypoventilation syndrome (Ondine's curse). *Nat Genet* 33:459–461.
14. Trochet D, *et al*. (2005) Molecular consequences of PHOX2B missense, frameshift and alanine expansion mutations leading to autonomic dysfunction. *Hum Mol Genet* 14:3697–3708.
15. Weese-Mayer DE, Berry-Kravis EM, Marazita ML (2005) In pursuit (and discovery) of a genetic basis for congenital central hypoventilation syndrome. *Respir Physiol Neurobiol* 149:73–82.
16. Kumar R, *et al*. (2005) Neuroanatomic deficits in congenital central hypoventilation syndrome. *J Comp Neurol* 487:361–371.
17. Bachetti T, *et al*. (2006) Brainstem anomalies in two patients affected by congenital central hypoventilation syndrome. *Am J Respir Crit Care Med* 174:706–709.
18. Harper RM, *et al*. (2005) Hypercapnic exposure in congenital central hypoventilation syndrome reveals CNS respiratory control mechanisms. *J Neurophysiol* 93:1647–1658.
19. Gonzalez C, Almaraz L, Obeso A, Rigual R (1994) Carotid body chemoreceptors: From natural stimuli to sensory discharges. *Physiol Rev* 74:829–898.
20. Katz DM, Finley JC, Polak J (1993) Dopaminergic and peptidergic sensory innervation of the rat carotid body: Organization and development. *Adv Exp Med Biol* 337:43–49.
21. Hilaire G, Viemari JC, Coulon P, Simonneau M, Bevengut M (2004) Modulation of the respiratory rhythm generator by the pontine noradrenergic A5 and A6 groups in rodents. *Respir Physiol Neurobiol* 143:187–197.
22. Smith JC, Ellenberger HH, Ballanyi K, Richter DW, Feldman JL (1991) Pre-Bötzinger complex: A brainstem region that may generate respiratory rhythm in mammals. *Science* 254:726–729.
23. Feldman JL, Del Negro CA (2006) Looking for inspiration: New perspectives on respiratory rhythm. *Nat Rev Neurosci* 7:232–242.
24. Richter DW, Manzke T, Wilken B, Ponimaskin E (2003) Serotonin receptors: Guardians of stable breathing. *Trends Mol Med* 9:542–548.
25. Gray PA, Rekling JC, Bocchiaro CM, Feldman JL (1999) Modulation of respiratory frequency by peptidergic input to rhythmogenic neurons in the preBötzinger complex. *Science* 286:1566–1568.
26. Gray PA, Janczewski WA, Mellen N, McCrimmon DR, Feldman JL (2001) Normal breathing requires preBötzinger complex neurokinin-1 receptor-expressing neurons. *Nat Neurosci* 4:927–930.
27. Jacquin TD, *et al*. (1996) Reorganization of pontine rhythmogenic neuronal networks in *Krox-20* knock-out mice. *Neuron* 17:747–758.
28. del Toro ED, *et al*. (2001) Generation of a novel functional neuronal circuit in Hoxa1 mutant mice. *J Neurosci* 21:5637–5642.
29. Shirasawa S, *et al*. (2000) Rnx deficiency results in congenital central hypoventilation. *Nat Genet* 24:287–290.
30. Qian Y, *et al*. (2001) Formation of brainstem (nor)adrenergic centers and first-order relay visceral sensory neurons is dependent on homeodomain protein Rnx/Tlx3. *Genes Dev* 15:2533–2545.
31. Viemari JC, *et al*. (2004) Phox2a gene, A6 neurons, and noradrenaline are essential for development of normal respiratory rhythm in mice. *J Neurosci* 24:928–937.
32. Morin X, *et al*. (1997) Defects in sensory and autonomic ganglia and absence of locus coeruleus in mice deficient for the homeobox gene *Phox2a*. *Neuron* 18:411–423.
33. Blanchi B, *et al*. (2003) MafB deficiency causes defective respiratory rhythmogenesis and fatal central apnea at birth. *Nat Neurosci* 6:1091–1100.
34. Guo H, Hellard DT, Huang L, Katz DM (2005) Development of pontine noradrenergic A5 neurons requires brain-derived neurotrophic factor. *Eur J Neurosci* 21:2019–2023.
35. Erickson JT, *et al*. (1996) Mice lacking brain-derived neurotrophic factor exhibit visceral sensory neuron losses distinct from mice lacking NT4 and display a severe developmental deficit in control of breathing. *J Neurosci* 16:5361–5371.
36. Amiel J, Trochet D, Clement-Ziza M, Munnich A, Lyonnet S (2004) Polyalanine expansions in human. *Hum Mol Genet* 13(Spec No 2):R235–R243.
37. Brown LY, Brown SA (2004) Alanine tracts: The expanding story of human illness and trinucleotide repeats. *Trends Genet* 20:51–58.
38. Dauger S, *et al*. (2003) Phox2b controls the development of peripheral chemoreceptors and afferent visceral pathways. *Development (Cambridge, UK)* 130:6635–6642.
39. Nattie EE (2001) Central chemosensitivity, sleep, and wakefulness. *Respir Physiol* 129:257–268.
40. Oren J, Kelly DH, Shannon DC (1987) Long-term follow-up of children with congenital central hypoventilation syndrome. *Pediatrics* 80:375–380.
41. Antic NA, *et al*. (2006) PHOX2B mutation-confirmed congenital central hypoventilation syndrome: Presentation in adulthood. *Am J Respir Crit Care Med* 174:923–927.
42. Lallemand Y, Luria V, Haffner-Krausz R, Lonai P (1998) Maternally expressed PGK-Cre transgene as a tool for early and uniform activation of the Cre site-specific recombinase. *Transgenic Res* 7:105–112.
43. Matrot B, *et al*. (2005) Automatic classification of activity and apneas using whole body plethysmography in newborn mice. *J Appl Physiol* 98:365–370.
44. Ramanantsoa N, *et al*. (2006) Ventilatory response to hyperoxia in newborn mice heterozygous for the transcription factor Phox2b. *Am J Physiol Regul Integr Comp Physiol* 290:R1691–R1696.
45. Abercrombie M (1946) Estimation of nuclear population from microtome sections. *Anat Rec* 94:239–247.
46. Guillery RW, Herrup K (1997) Quantification without pontification: Choosing a method for counting objects in sectioned tissues. *J Comp Neurol* 386:2–7.
47. Dufour HD, *et al*. (2006) Pre-craniate origin of cranial motoneurons. *Proc Natl Acad Sci USA* 103:8727–8732.
48. Hirsch M-R, Glover J, Dufour HD, Brunet J-F, Goridis C (2007) Forced expression of Phox2 homeodomain transcription factors induces a branchio-visceromotor axonal phenotype. *Dev Biol* 303:687–702.
49. Pattyn A, Morin X, Cremer H, Goridis C, Brunet J-F (1997) Expression and interactions of the two closely related homeobox genes Phox2a and Phox2b during neurogenesis. *Development (Cambridge, UK)* 124:4065–4075.
50. Fisher JT, Mortola JP, Smith JB, Fox GS, Weeks S (1982) Respiration in newborns. *Am Rev Respir Dis* 125:650–657.